

Domain wall roughness in epitaxial ferroelectric $\text{PbZr}_{0.2}\text{Ti}_{0.8}\text{O}_3$ thin films

P. Paruch, T. Giamarchi, and J.-M. Triscone

DPMC, University of Geneva, 24 Quai E. Ansermet, 1211 Geneva 4, Switzerland

(dated: March 22, 2024)

The static configuration of ferroelectric domain walls was investigated using atomic force microscopy on epitaxial $\text{PbZr}_{0.2}\text{Ti}_{0.8}\text{O}_3$ thin films. Measurements of domain wall roughness reveal a power law growth of the correlation function of relative displacements $B(L)/L^2$ with $\alpha = 0.26$ at short length scales L , followed by an apparent saturation at large L . In the same films, the dynamic exponent was found to be 0.6 from independent measurements of domain wall creep. These results give an effective domain wall dimensionality of $d = 2.5$, in good agreement with theoretical calculations for a two-dimensional elastic interface in the presence of random-bond disorder and long range dipolar interactions.

PACS numbers: 77.80.-e, 77.80.Dj, 77.80.Fm

Understanding the behavior of elastic objects pinned by periodic or disorder potentials is of crucial importance for a large number of physical systems ranging from vortex lattices in type II superconductors [1], charge density waves [2] and Wigner crystals [3] to interfaces during growth [4] and fluid invasion [5] processes, and magnetic domain walls [6]. Ferroelectric materials, whose switchable polarization and piezoelectric and pyroelectric properties make them particularly promising for applications such as non-volatile memories [7, 8], actuators, and sensors [10], are another such system. In these materials, regions with different symmetry-equivalent ground states characterized by a stable remanent polarization are separated by elastic domain walls. The application of an electric field favors one polarization state by reducing the energy necessary to create a nucleus with polarization parallel to the field, and thereby promotes domain wall motion. Since most of the proposed applications use multi-domain configurations, understanding the mechanisms that control domain wall propagation and pinning in ferroelectrics is an important issue.

A phenomenological model derived from measurements of domain growth in bulk ferroelectrics [11, 12, 13] initially suggested that the domain walls were pinned by the periodic potential of the crystal lattice itself. Such pinning was deemed possible because of the extreme thinness of ferroelectric domain walls (different from the case of magnetic systems). However, measurements of the piezoelectric effect [22], dielectric permittivity [23], and dielectric dispersion [24] in ferroelectric ceramics and sol-gel films have shown some features which cannot be described by the existing phenomenological theories. A microscopic study of ferroelectric domain walls could resolve these issues. Recently, we have measured domain wall velocity in epitaxial $\text{PbZr}_{0.2}\text{Ti}_{0.8}\text{O}_3$ thin films, showing that in this case commensurate lattice pinning is in fact not the dominant mechanism [14, 15]. Rather, a creep-like velocity (v) response to an externally applied electric field E was observed with $v \propto \exp[C/E]$, where C is a constant. The exponent characterizing the dynamic

behavior of the system is a function of the domain wall dimensionality and the nature of the pinning potential. These results suggested that domain wall creep in ferroelectric films is a disorder-controlled process. However, questions about the microscopic nature of the disorder were left open by the dynamical measurements alone. In order to ascertain the precise physics of the pinned domain walls and also the possible role of the long-range dipolar interactions which exist in ferroelectric materials, it is thus necessary to perform a direct analysis of the static domain wall configuration, extracting the roughness exponent and the effective domain wall dimensionality d_e . Although measurements of this kind have been performed on other elastic disordered systems such as vortices (using neutron diffraction and decoration) [16, 17], charge density waves (using X-ray diffraction) [18], contact lines [19], and ferromagnetic domain walls [6], a successful comparison between the experimentally observed roughness exponent and theoretical predictions could only be carried out in magnetic systems. In these systems, good agreement with the value $\alpha = 2/3$ predicted for one-dimensional (line) domain walls in a random bond disorder was found [6]. Quantitative studies of these phenomena in other microscopic systems are therefore clearly needed. Epitaxial perovskite ferroelectric thin films with high crystalline quality and precisely controllable thickness are an excellent model system for such studies.

In this paper we report on the first direct measurement of ferroelectric domain wall roughness. To image ferroelectric domains with the nanometer resolution required by such studies, atomic force microscopy (AFM) was used [14, 15, 20, 21]. Relaxation of the domain walls to their equilibrium configuration at short length scales allowed us to obtain values of $\alpha = 0.26$ for the roughness exponent. In the same films, the dynamic exponent was found to be 0.5 (0.6 from independent measurements of domain wall creep). An analysis of these results gives an effective dimensionality of $d = 2.5$ for the domain walls, in good agreement with theoretical calculations for a two-

dimensional elastic interface in the presence of random - bond disorder and long range dipolar interactions [25].

The ferroelectric domain wall roughness studies were carried out in three c-axis oriented $\text{PbZr}_{0.2}\text{Ti}_{0.8}\text{O}_3$ films, 50, 66 and 91 nm thick, epitaxially grown on single crystalline (001) Nb:SrTiO_3 substrates by radio-frequency magnetron sputtering, as detailed in ref. [26, 27]. In these films, the polarization vector is parallel or anti-parallel to the c-axis and can be locally switched by the application of voltage signals via a metallic AFM tip, using the conductive substrate as a ground electrode [28, 29]. The resulting ferroelectric domains are imaged by piezoelectric microscopy (PFM) [28]. To measure domain wall roughness, we wrote linear domain structures with alternating polarization by applying alternating 12 V signals while scanning the AFM tip in contact with the film surface. We chose line widths of 1 { 1.5 μm , and lengths of 8 { 15 μm to ensure that domain wall images (2.5 { 2.5 and 5 { 5 μm^2) used in the study could be taken in the central regions, away from possible edge effects. Multiple domain structures were written in photolithographically pre-defined areas on each sample. More than 100 different ferroelectric domain walls were written and imaged in the three films.

From these measurements, we extracted the correlation function of relative displacements

$$B(L) = \overline{h[u(z+L) - u(z)]^2} \quad (1)$$

where the displacement vector $u(z)$ measures the deformation of the domain wall from an elastically optimal configuration due to pinning in favorable regions of the potential landscape. h and $\overline{}$ denote the thermodynamic and ensemble disorder averages, respectively. Experimentally, the latter is realized by averaging over all pairs of points separated by the fixed distance L , ranging from 1 to 500 pixels (5 or 10 nm { 2.5 or 5.0 μm , depending on the image size) in our measurements. As shown in Fig. 1 for the three different films used, we observe a power-law growth of $B(L)$ at short length scales, comparable to the 50 { 100 nm film thickness, followed by saturation of $B(L)$ in the 100 { 1000 nm^2 range [35]. The observed $B(L)$ saturation indicates that the walls do not relax at large length scales from their initial straight configuration, dictated by the position of the AFM tip during writing. To ensure that domain wall relaxation was not hindered by the pinning planes of the lattice potential in the ferroelectric films [30, 31], we wrote sets of domain walls at different orientations with respect to the crystalline axes in the 66 nm film. We found no correlation between the roughness of domain walls and their orientation in the crystal. This result is in agreement with previous studies [14] pointing out the negligible role of the commensurate potential compared to the effects of disorder.

To investigate the possibility of thermal relaxation at ambient conditions, we then measured a set of domain

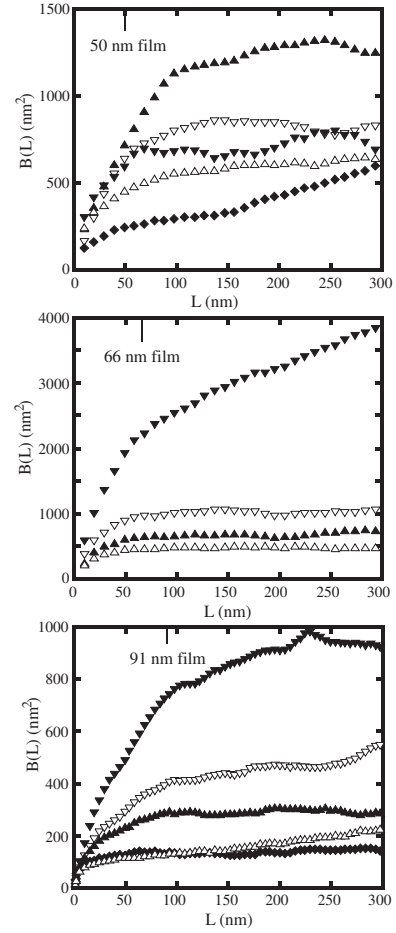


FIG. 1: Average displacement correlation function $B(L)$ for different sets of ferroelectric domain walls in 50 (a), 66 (b) and 91 (c) nm thick films, shown out to $L = 300$ nm. Power law growth of $B(L)$ is observed at short length scales, followed by saturation, suggesting a non-equilibrium configuration at large L .

walls over a period of 1 month. No relaxation from the as-written configuration at large L is apparent visually (Fig. 2(a)), or when comparing $B(L)$ extracted for this set of domain walls at different times (Fig. 2(b)). These data strongly indicate that ambient thermal activation alone is not sufficient to equilibrate the domain walls over their entire length [36]. These results are in agreement with our previous studies [9, 15] in which both linear and nanoscopic circular domains remained completely stable over 1 { 5 month observation periods. Such high stability is inherent to the physics of an elastic disordered system, where energy barriers between different metastable states diverge as the electric field driving domain wall motion goes to zero. This is an advantage for possible memory or novel filter applications [9], but also makes relaxation exceedingly slow. In fact, we believe that even the relaxation leading to the observed power-law growth of $B(L)$ at smaller length scales is not

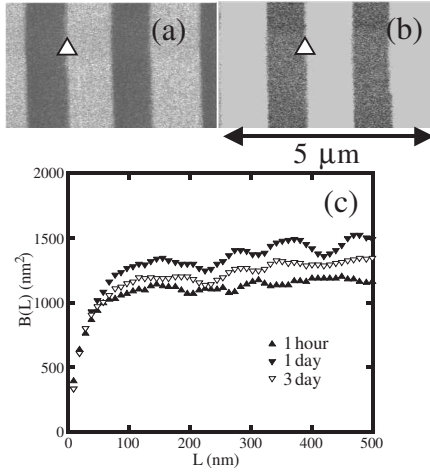


FIG. 2: PFM images of the same set of domain walls taken (a) 1 hour after writing and (b) 1 week later. The white triangle indicates the same domain wall in each image. (c) The average $B(L)$ for this set of domain walls.

purely thermal, but occurs during the writing process itself. When the direction of the applied electric field is reversed to form the alternating domain structure, the neighboring region already written with the opposite polarity nonetheless experiences the resulting electric field, allowing the domain wall to locally reach an equilibrium configuration.

From the power-law growth of $B(L)$ at these short length scales, we extract a value for the roughness exponent ζ . This exponent characterizes the roughness of the domain wall in the random manifold regime where an interface individually optimizes its energy with respect to the disorder potential landscape and $B(L)$ scales as $B(L) \propto L^{2\zeta}$. As shown in Fig. 3(a), a linear fit of the lower part of the $\ln(B(L))$ vs $\ln(L)$ curve allows ζ to be determined. Average values of $\zeta = 0.26, 0.29$ and 0.22 were obtained for the 50, 66 and 91 nm thick films, respectively, indicated by the horizontal lines in Fig. 3(b).

In addition to the investigations of static domain wall roughness described above, we independently measured domain wall dynamics in each film, using the approach detailed in [14, 15]. As shown in Fig. 4, we observe the non-linear velocity response to applied electric fields characteristic of a creep process, with values of 0.59, 0.58 and 0.51 for the dynamical exponent ν in the 50, 66 and 91 nm thick films, respectively [37].

When these data are analyzed in the theoretical framework of a disordered elastic system, they provide information on the microscopic mechanism governing domain wall behavior. The direct measurement of domain wall roughness clearly rules out the lattice potential as a dominant source of pinning. In that case, the walls would have been flat with $B(L) \propto L^2$, where the lattice spacing $a \approx 4$ Å is the period of the pinning potential [31].

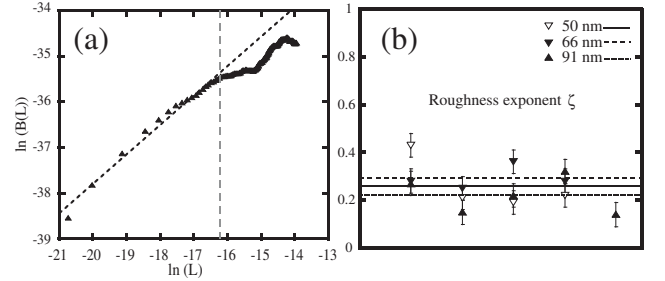


FIG. 3: (a) Typical \ln - \ln plot of $B(L)$. Fitting the linear part of the curve (left of the vertical line) gives ζ . (b) Average values of the characteristic roughness exponent extracted from the equilibrium portion of the $B(L)$ data are 0.26, 0.29 and 0.22 in the 50, 66 and 91 nm thick samples, respectively, indicated by the horizontal lines in the figure.

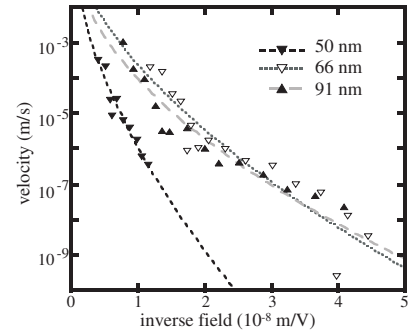


FIG. 4: Domain wall speed as a function of the inverse applied electric field extracted from measurements of domain growth in the 50, 66 and 91 nm thick films. The data fit well to $v \propto \exp[-C/E]$ with $\nu = 0.59, 0.58$ and 0.51 , respectively.

Given the stability and reproducibility of the wall position over time, shown in Fig. 2, the effect of thermal relaxation on the observed increase of $B(L)$ can also be ruled out. The measured roughness must thus be attributed to disorder. Two disorder universality classes exist, with different roughness exponents. Random bond disorder, corresponding to defects maintaining the symmetry of the two polarization states would change only the local depth of the ferroelectric double well potential. Theoretically, this disorder would lead to a roughness exponent $\zeta_{RB} = 2/3$ in $d_e = 1$ and $\zeta_{RB} = 0.2084(4)$ for other dimensions. Random field disorder, corresponding to defects which locally asymmetrize the ferroelectric double well would favor one polarization state over the other. Such disorder would lead to a roughness exponent $\zeta_{RF} = (4 - d_e)/3$ in all dimensions below four. Should the wall be described by standard (short range) elasticity, d_e in the above formulas is simply the dimension d of the domain wall ($d = 1$ for a line, $d = 2$ for a sheet). However, in ferroelectrics the stiffness of the domain walls and thus their elasticity under deformations in the direction of polarization is different from the one for deformations perpendicular to the direction of polarization be-

cause of long range dipolar interactions [25]. The elastic energy (expressed in reciprocal space) thus contains not only a short range term $H = \frac{1}{2} \sum_q C_{el}(q) u(q) u(q)$ with $C_{el} = \omega q^2$ but also a correction term due to the dipolar interaction $C_{dp} = \frac{2P_s^2 q_y^2}{\epsilon_0} + \frac{P_s^2}{\epsilon_0} \frac{3}{4} q_x^2 + \frac{1}{8} q^2$ where y is the direction of the polarization. P is the ferroelectric polarization and ϵ_0 and ϵ_r are the relative and vacuum dielectric constants. Because q_y now scales as $q_y \propto q_x^{3/2}$, the effective dimension d_e to use in the above formulas is $d_e = d + 1 = 2$ [25, 32]. Using the above expressions for the roughness exponent we see that the measured 0.26 value would give $d_e = 3$ for random field disorder, ruling out this scenario. On the other hand random bond disorder would give $d_e = 2.5$ to 2.9, a much more satisfactory value, which is compatible with a scenario of two-dimensional walls (sheets) in random bond disorder with long range dipolar interactions.

This conclusion can be independently verified by the dynamic measurements, since the creep exponent is related to the static roughness exponent via $\mu = \frac{d_{eff} - 2}{2}$. The values of these two exponents from the independent static and dynamic measurements can therefore be used to calculate d_e . For the 50, 66 and 91 nm thick $\text{Pb}_{0.98}\text{Zr}_{0.02}\text{Ti}_{0.98}\text{O}_3$ films we find $\mu = 2.42, 2.49$ and 2.47 , respectively, in very good agreement with the expected theoretical value for a two-dimensional elastic interface in the presence of disorder and dipolar interactions. Taken together, these two independent analyses provide strong evidence that the pinning in thin ferroelectric films is indeed due to disorder in the random bond universality class. The precise microscopic origin of such disorder is still to be determined. Preliminary studies of domain wall dynamics in pure PbTiO_3 films gave comparable results to those for $\text{Pb}_{0.98}\text{Zr}_{0.02}\text{Ti}_{0.98}\text{O}_3$, suggesting that the presence of Zr in the solid solution is not a dominant factor, and that other defects presumably play a more significant role. Note that for the short-range domain wall relaxation observed, the walls are in the two-dimensional limit. However, if equilibrium domain wall roughness could be measured for larger L , a crossover to one-dimensional behavior would be expected, with a roughness exponent $\mu = 2/3$.

In conclusion, we used AFM measurements of high quality epitaxial $\text{Pb}_{0.98}\text{Zr}_{0.02}\text{Ti}_{0.98}\text{O}_3$ thin films to obtain the roughness exponent for ferroelectric domain walls. This is the first direct observation of static domain wall roughness in ferroelectric systems, and, combined with our measurements of domain wall dynamics, provides a coherent physical image of their behavior in the framework of elastic disordered systems.

This work was supported by the Swiss National Science Foundation through the National Center of Competence in Research "Materials with Novel Electronic Properties - MAnEP" and Division II. Further support was provided by the New Energy and Industrial Technology Development Organization (NEDO) and the European Science

Foundation (THOX).

-
- [1] G. B. Latter, et al., Rev. Mod. Phys. 66, 1125 (1994).
 - [2] G. G. Guner, Rev. Mod. Phys. 60, 1129 (1988).
 - [3] E. Y. Andrei et al., Phys. Rev. Lett. 60, 2765 (1988).
 - [4] M. Kardar, Physica B Special Issue (to be published), 1995.
 - [5] D. W. Ilkenson and J. F. Willemsen, J. Phys. A 16, 3365 (1983).
 - [6] S. Lemler, et al., Phys. Rev. Lett. 80, 849 (1998).
 - [7] J. F. Scott and C. A. Araujo, Science 246, 1400 (1989).
 - [8] R. Waser and A. Rudiger, Nature Mater. 3, 81 (2004).
 - [9] A. K. S. Kumar, et al., Appl. Phys. Lett. 85, 1757 (2004).
 - [10] C. Caliendo, I. Fratoddi, and M. V. Russo, Appl. Phys. Lett. 80, 4849 (2002).
 - [11] R. C. Miller and G. Weinreich, Phys. Rev. 117, 1460 (1960).
 - [12] W. J. Merz, Phys. Rev. 95, 690 (1954).
 - [13] F. Fatuzzo and W. J. Merz, Phys. Rev. 116, 61 (1959).
 - [14] T. Tybell, P. Paruch, T. Giamarchi, and J.-M. Triscone, Phys. Rev. Lett. 89, 097601 (2002).
 - [15] P. Paruch, T. Giamarchi, T. Tybell, and J.-M. Triscone, 2004, cond-mat/0411178.
 - [16] P. Kim, Z. Yao, C. A. Bolle, and C. M. Lieber, Phys. Rev. B 60, R12589 (1999).
 - [17] T. Klein, et al., Nature 413, 404 (2001).
 - [18] S. Rouzic, S. Ravy, J.-P. Pouget, and S. Brazovskii, Phys. Rev. B 62, R16231 (2000).
 - [19] S. Moullet, C. Guthmann, and E. Rolley, Eur. Phys. J. E 8, 437 (2002).
 - [20] P. Paruch, T. Tybell, and J.-M. Triscone, Appl. Phys. Lett. 79, 530 (2004).
 - [21] Y. Cho, et al., Appl. Phys. Lett. 81, 4401 (2002).
 - [22] D. Damjanovic, Phys. Rev. B 55, R649 (1997).
 - [23] D. V. Taylor and D. Damjanovic, Appl. Phys. Lett. 73, 2045 (1998).
 - [24] V. Mueller, et al., Phys. Rev. B 65, 134102 (2002).
 - [25] T. Nattermann, J. Phys. C 16, 4125 (1983).
 - [26] T. Tybell, C. H. Ahn, and J.-M. Triscone, Appl. Phys. Lett. 72, 1454 (1998).
 - [27] J.-M. Triscone, et al., J. Appl. Phys. 79, 4298 (1996).
 - [28] P. Guthner and K. D. Ransfeld, Appl. Phys. Lett. 61, 1137 (1992).
 - [29] C. H. Ahn, et al., Science 276, 1100 (1997).
 - [30] S. Poykko and D. J. Chadi, Appl. Phys. Lett. 75, 2830 (1999).
 - [31] B. Meyer and D. Vanderbilt, Phys. Rev. B 65, 104111 (2002).
 - [32] T. Emig and T. Nattermann, Eur. Phys. J. B 8, 525 (1999).
 - [33] U. Yaron, et al., Phys. Rev. Lett. 73, 2748 (1994).
 - [34] I. Joumard, et al., Physica C 377, 165 (2002).
 - [35] This saturation is apparent well below $L = 1.25$ or 2.5 nm, the limit at which the finite size of the image begins to play a role.
 - [36] In other elastic disordered systems relaxation was achieved by the applying small oscillating driving forces [33, 34], or by subcritically driving the manifold into an equilibrium configuration [6]. Using Pt electrodes deposited on top of the writing areas we therefore applied

both DC and AC voltages to different domain structures. Unfortunately, the large degree of leakage in such thin InSb , avoided in the local probe configuration, did not allow the domain walls to reach equilibrium at large L , with no relaxation observed when comparing $B(L)$ for

domain wall imaged before and after voltage application. [37] These values are lower than the three values measured in [14], but consistent with all the subsequent measurements performed on nine other InSb , all grown under similar conditions.